Channeling Quantum Criticality

Yijian Zou,[1] Shengqi Sang,[2,3] and Timothy H. Hsieh[2]
[1]*Stanford Institute for Theoretical Physics, Stanford University, Stanford, California 94305, USA*
[2]*Perimeter Institute for Theoretical Physics, Waterloo, Ontario N2L 2Y5, Canada*
[3]*University of Waterloo, Waterloo, Ontario N2L 3G1, Canada*

(Received 3 February 2023; revised 22 March 2023; accepted 24 May 2023; published 21 June 2023)

We analyze the effect of decoherence, modeled by local quantum channels, on quantum critical states and we find universal properties of the resulting mixed state's entanglement, both between system and environment and within the system. Renyi entropies exhibit volume law scaling with a subleading constant governed by a "g function" in conformal field theory, allowing us to define a notion of renormalization group (RG) flow (or "phase transitions") between quantum channels. We also find that the entropy of a subsystem in the decohered state has a subleading logarithmic scaling with subsystem size, and we relate it to correlation functions of boundary condition changing operators in the conformal field theory. Finally, we find that the subsystem entanglement negativity, a measure of quantum correlations within mixed states, can exhibit log scaling or area law based on the RG flow. When the channel corresponds to a marginal perturbation, the coefficient of the log scaling can change continuously with decoherence strength. We illustrate all these possibilities for the critical ground state of the transverse-field Ising model, in which we identify four RG fixed points of dephasing channels and verify the RG flow numerically. Our results are relevant to quantum critical states realized on noisy quantum simulators, in which our predicted entanglement scaling can be probed via shadow tomography methods.

DOI: 10.1103/PhysRevLett.130.250403

Introduction.—Quantum devices have advanced significantly to the point of challenging classical computers in sampling and simulation tasks [1–5]. In the context of quantum many-body physics, they are promising experimental platforms for realizing long-range entangled quantum phases of matter including topological order [6,7] and quantum critical states [8]. Furthermore, their controllability at the single-qubit level enables the exploration of quantum dynamics beyond simple time evolution with a Hamiltonian, and one prominent example is dynamics involving both unitary evolution and projective measurements [9–15]. Nevertheless, quantum devices are noisy and any states prepared are subject to decoherence. One important question is which properties of quantum matter survive in a noisy environment, and how does one understand any residual order in the mixed state? Recently, substantial progress has been made in understanding mixed state versions of gapped quantum systems including symmetry protected topological phases and topological order [16–23].

In this work, we study quantum critical states under decoherence, modeled by local quantum channels. A point of inspiration is prior work [24–27] which found that measurements (with outcomes recorded) can have a significant effect on quantum critical states, in some cases boosting long-range correlation. However, verifying such effects typically requires postselecting on monitored pure state trajectories. In contrast, quantum channels can be viewed as an environmental measurement in which the outcomes are averaged over, and we are interested in properties of the resulting mixed state, thus avoiding the need for postselection.

Naively one might expect that local quantum channels cannot induce new universality classes since they can be represented as finite depth unitaries acting on an enlarged Hilbert space, and such finite depth unitaries cannot change the nature of long-distance correlations. While this is true for local, linear observables of the state, nonlinear quantities like entanglement measures can be significantly affected by local channels.

Indeed, a key finding of our work is that for entanglement measures like Renyi entropies and entanglement negativity, local quantum channels acting on quantum critical states can drive phase transitions or, more technically, renormalization group (RG) flows, between different conformal fixed points labeling different quantum channels. More specifically, we find that in computing such measures, quantum channels map to boundary conditions for multiple copies of the original conformal field theory (CFT) describing the critical state. Under coarse graining, such boundary conditions can flow to a variety of conformal fixed points whose classification can be much richer than that of the single copy CFT.

Concretely, we find that the Renyi entropy of the decohered state, which quantifies the entanglement between system and environment, is extensive but has a subleading

 © 2023 American Physical Society

term dictated by a "g function" in CFT. This g function characterizes the channel with respect to Renyi entropy and dictates the direction of RG flow between two channels: a channel with a larger g can flow to a channel with smaller g if weakly perturbed by the latter. Moreover, near a RG fixed point, the g function has a universal scaling form determined by critical exponents. One natural consequence of our formalism is that the Renyi entropy of a subsystem A of the decohered state has a subleading logarithmic scaling with $|A|$ and its coefficient is given by scaling dimensions of certain boundary condition changing operators. Furthermore, Renyi negativity of the subsystem (a measure of entanglement within the mixed state) can obey either logarithmic scaling or area law based on the universal properties of the RG fixed point. In the former case, the coefficient of log scaling can either change continuously with decoherence strength or remain the same as the initial pure critical state, depending on whether the channel corresponds to a marginal or irrelevant perturbation, respectively. We demonstrate all these features for the one-dimensional transverse-field Ising critical point and conclude with a discussion of experimental relevance to quantum simulators.

Quantum channels.—We first review useful facts about quantum channels [28]. A quantum channel represents the most general quantum process including decoherence. Formally, it is a completely positive trace-preserving map $\rho \to \mathcal{N}(\rho)$ acting on density matrices. For a quantum channel, one may define its dual channel $\mathcal{N}^*$, which is a linear map on operators satisfying $\mathrm{Tr}[\rho\mathcal{N}^*(O)] = \mathrm{Tr}[\mathcal{N}(\rho)O]$, $\forall\, O$.

Here we consider a spatially uncorrelated noise model defined on a qubit chain. The noise can be modeled as a product of single-qubit channels $\mathcal{N} = \otimes_{j=1}^{L} \mathcal{N}_j$, where each $\mathcal{N}_j$ is a channel acting on the jth qubit.

We focus on the dephasing channel $\mathcal{N}_j = \mathcal{D}^{[j]}_{p,\vec{v}}$, which represents an environment-qubit coupling with the jth system qubit along the $\sigma_{\vec{v}} \coloneqq v_x\sigma_x + v_y\sigma_y + v_z\sigma_z$ direction. The action of $\mathcal{D}^{[j]}_{p,\vec{v}}$ on the density matrix ρ of a qubit is

$$\mathcal{D}^{[j]}_{p,\vec{v}}(\rho) = \left(1 - \frac{p}{2}\right)\rho + \frac{p}{2}\sigma^{[j]}_{\vec{v}}\rho\sigma^{[j]}_{\vec{v}}. \tag{1}$$

The channel is self-dual; i.e., $\mathcal{D}^{[j]*}_{p,\vec{v}} = \mathcal{D}^{[j]}_{p,\vec{v}}$. The parameter $p \in [0, 1]$ controls the strength of the noise: when $p = 0$, it is the identity channel and leaves states unchanged; while if $p = 1$, it turns any quantum state into a classical ensemble.

General formalism mapping information-theoretic quantities to quantum quench problem.—We consider a critical ground state $|\psi\rangle$ under decoherence of the above type, resulting in density matrix $\rho = \mathcal{N}(|\psi\rangle\langle\psi|)$. We study information-theoretic quantities including nth-Renyi entropy and entanglement negativity, and we map these quantities to quantum quench problems in $\mathrm{CFT}^{\otimes 2n}$, i.e., a $2n$-copied CFT.

We start with the Renyi entropy of a subsystem A: $S^{(n)}_A(\rho) \coloneqq (1/(1-n)) \log \mathrm{Tr}(\rho^n_A)$, where $\rho_A = \mathrm{Tr}_{\bar{A}}\rho$. This is a measure of both quantum and classical correlation between A and the rest of the system $\bar{A}$ together with the environment. It reduces to the von Neumann entropy after taking the replica limit $n \to 1$. The partition function $Z^{(n)}_A \coloneqq \mathrm{Tr}(\rho^n_A)$ can be rewritten as

$$Z^{(n)}_A = \mathrm{Tr}(\rho^{\otimes n}\tau_{n,A}) = \mathrm{Tr}[\mathcal{N}(|\psi\rangle\langle\psi|)^{\otimes n}\tau_{n,A}], \tag{2}$$

where $\tau_{n,A} = \prod_{j\in A}\tau_{n,j}$ forward permutes the replicas for sites in A, and acts as identity for sites in $\bar{A}$. Next, we use the dual channel to rewrite

$$Z^{(n)}_A = \mathrm{Tr}[(|\psi\rangle\langle\psi|)^{\otimes n}B_{\mathcal{N},A}], \tag{3}$$

where $B_{\mathcal{N},A} \coloneqq \mathcal{N}^{*\otimes n}(\tau_{n,A}) = \otimes_{j\in A}\mathcal{N}^{*\otimes n}_j(\tau_{n,j})$. Finally, we use the standard folding trick for defect CFT [29] to treat each operator O as a state $|O\rangle\rangle$ in the doubled Hilbert space, whose inner product is defined as $\langle\langle O_1|O_2\rangle\rangle = \mathrm{Tr}(O_1^\dagger O_2)$. Thus, under the folding,

$$Z^{(n)}_A = \langle\langle(\psi \otimes \psi^*)^{\otimes n}|B_{\mathcal{N},A}I_{\bar{A}}\rangle\rangle. \tag{4}$$

The bra state $|(\psi\otimes\psi^*)^{\otimes n}\rangle\rangle$ is $2n$ copies of the critical state, while the ket state $|B_{\mathcal{N}}\rangle\rangle$ is a product state, since the operator $B_{\mathcal{N},A}$ factorizes among j. Thus, we have reformulated the Renyi entropy as a quantum quench problem from a product state $|B_{\mathcal{N}}\rangle\rangle$ to a $2n$-copied CFT, whose path integral representation on the spacetime manifold is shown in Fig. 1 (top).

The other quantity that we consider is nth (n is odd) Renyi entanglement negativity $N^{(n)}_A(\rho) \coloneqq (1/(1-n)) \log(\mathrm{Tr}(\{\rho^{T_A}\}^n)/\mathrm{Tr}(\rho^n))$ for a subsystem A, where $(\cdot)^{T_A}$ is the partial-transpose operation that swaps the bra and ket

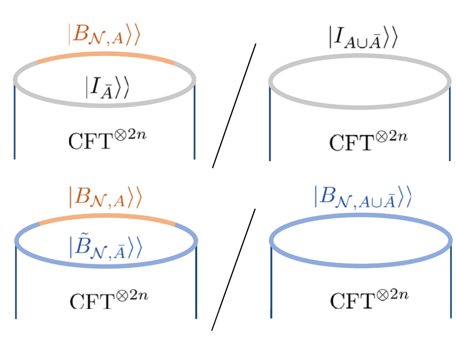

FIG. 1. Entanglement quantities of decohered critical state involve overlaps between copies of CFT and boundary states determined by the quantum channel (see main text). Top: path integral representation of partition function used to compute Renyi entropy Eq. (4). Note that the denominator is $\langle\psi^{\otimes n}|\psi^{\otimes n}\rangle = 1$. Bottom: path integral representation of the analogous object for Renyi negativity Eq. (5).

states in ρ for sites within A. $N_A^{(n)}$ is a measure of *quantum* correlation between A and the rest of the system $\bar{A}$ [30,31]. A similar derivation shows that

$$N_A^{(n)}(\rho) = \frac{1}{1-n}\log\frac{\langle\langle(\psi\otimes\psi^*)^{\otimes n}|B_{\mathcal{N},A}\tilde{B}_{\mathcal{N},\bar{A}}\rangle\rangle}{\langle\langle(\psi\otimes\psi^*)^{\otimes n}|B_{\mathcal{N},A\cup\bar{A}}\rangle\rangle}, \quad (5)$$

where $\tilde{B}_{\mathcal{N},\bar{A}} = \otimes_{j\in\bar{A}}\mathcal{N}_j^{*\otimes n}(\tau_{n,j}^{-1})$. Thus the calculation of $N_A^{(n)}$ is mapped to a quantum quench from another product initial state to the same $2n$-copied CFT; see Fig. 1 (bottom). In such quantum quench problems, it has been shown [32–35] that a short-range correlated state can be described by a conformal boundary condition at long distances. We will assume that this is the case for product states $|B_{\mathcal{N}}\rangle\rangle$ and $|\tilde{B}_{\mathcal{N}}\rangle\rangle$ [36].

The g function.—We now focus on the simplest quantity,

$$S^{(n)}(\rho) = \frac{1}{1-n}\log Z^{(n)}(L), \quad (6)$$

where L is the total system size. This is the Renyi entropy of the whole system or, alternatively, the Renyi entanglement entropy between system and environment. In a boundary CFT, the partition function $Z^{(n)}(L)$ depends on UV details, but one can define a UV-independent g function [48–50],

$$\log g^{(n)}(L) = \left(1 - L\frac{d}{dL}\right)\log Z^{(n)}(L), \quad (7)$$

which plays a similar role for boundary RG flow as the central charge c function plays for bulk RG flow. It satisfies the following two properties. First, $\log g^{(n)}(L)$ is a monotonically decreasing function of L. Second, for conformal boundary conditions (RG fixed points), $\log g^{(n)}(L) = \log g^{(n)}$ is independent of L, which equals the universal Affleck-Ludwig boundary entropy [51]. At these fixed points, solving the differential equation (7) gives $\log Z^{(n)}(L) = (1-n)\alpha^{(n)}L + \log g^{(n)}$, where $(1-n)\alpha^{(n)}$ is a nonuniversal integration constant. One of our main results,

$$S^{(n)}(\rho) = \alpha^{(n)}L - \frac{1}{n-1}\log g_{\mathcal{N}}^{(n)}, \quad (8)$$

then follows from Eq. (6). Given a lattice wave function, we may compute $g_{\mathcal{N}}^{(n)}(L)$ numerically using Eq. (7). We identify a channel $\mathcal{N}$ as a RG fixed point if $g_{\mathcal{N}}^{(n)}(L)$ becomes a constant $g_{\mathcal{N}}^{(n)}$ as L exceeds a few lattice spacings. The identity channel $\mathcal{I}$ is always a RG fixed point with $\log g_{\mathcal{I}}^{(n)} = 0$.

Let $\mathcal{N}_p$ be a family of quantum channels parametrized by p. We denote the g function of $\mathcal{N}_p$ as $g_p^{(n)}(L)$. Let $p = p_c$ be a RG fixed point with the g function g_c, then

$$g_p^{(n)}(L) = \bar{g}^{(n)}(|p-p_c|L^{1/\nu}), \quad (9)$$

where ν is the analog of the "correlation length exponent" in critical phenomena. If $\nu > 0$, then the fixed point $\mathcal{N}_{p_c}$ is unstable, and it flows into another fixed point with the g function $g' < g_c$. In such cases, the scaling function $\bar{g}^{(n)}$ is a monotonically decreasing function.

Subsystem entropy.—Now we consider the entropy of a subsystem, whose corresponding quantum quench problem is from a spatially inhomogeneous initial state; see Fig. 1 (top). Such an initial state can be described in CFT by inserting boundary condition changing operator $\phi_{\mathcal{IN}}^{(n)}$ and $\phi_{\mathcal{NI}}^{(n)} = \phi_{\mathcal{IN}}^{(n)*}$ at the intersections [52–54]. There are $2m$ insertions if A contains m disjoint intervals. In particular, if A is a single interval with length L_A, then the partition function $Z^{(n)}(L)$ is

$$\langle\phi_{\mathcal{IN}}^{(n)}(0)\phi_{\mathcal{IN}}^{(n)*}(L_A)\rangle = C\left(\frac{L}{\pi}\sin\frac{\pi L_A}{L}\right)^{-2\Delta_{\mathcal{IN}}^{(n)}}, \quad (10)$$

where $\Delta_{\mathcal{IN}}^{(n)}$ is the scaling dimension of $\phi_{\mathcal{IN}}^{(n)}$ and C is a normalization constant. Equation (10) together with Eq. (6) gives another main result [55]:

$$S^{(n)}(\rho_A) = \alpha^{(n)}L_A + \frac{2\Delta_{\mathcal{IN}}^{(n)}}{n-1}\log\left[\frac{L}{\pi}\sin\left(\frac{\pi L_A}{L}\right)\right] + O(1). \quad (11)$$

In order to numerically verify the formula, it is useful to consider the Renyi mutual information $I^{(n)}(A,B) = S^{(n)}(\rho_A) + S^{(n)}(\rho_B) - S^{(n)}(\rho_{AB})$. Choosing $B = \bar{A}$ to be the complement of A, we obtain

$$I^{(n)}(A,\bar{A}) = \frac{4\Delta_{\mathcal{IN}}^{(n)}}{n-1}\log\left[\frac{L}{\pi}\sin\left(\frac{\pi L_A}{L}\right)\right] + O(1), \quad (12)$$

in which the volume law pieces have canceled each other. Similar results hold for Renyi negativity $N_A^{(n)}(\rho)$, except that the boundary condition changing operator is different.

For two disjoint intervals $A = [x_1, x_2]$, $B = [x_3, x_4]$, we can show that $I^{(n)}(A,B)$ is only a function of the cross ratio $\eta = (X_{12}X_{34})/(X_{13}X_{24})$, where $X_{ij} = \sin(\pi|x_i - x_j|/L)$. At small η, we may fuse the two boundary condition changing operators $\phi_{\mathcal{IN}}^{(n)} \times \phi_{\mathcal{IN}}^{(n)*} = I + O^{(n)} + \cdots$, where $O^{(n)}$ is the second lowest operator in the operator product expansion. This implies the scaling:

$$I^{(n)}(A,B) = \text{const} \times \eta^{\Delta_O^{(n)}} \quad (\eta \ll 1). \quad (13)$$

Note that $O^{(n)}$ is a boundary operator at the boundary condition $|B_{\mathcal{I}}\rangle\rangle$, which we may unfold to get a bulk local

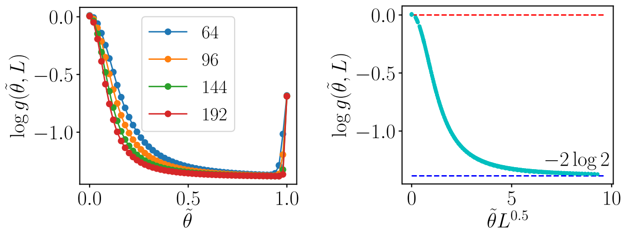

FIG. 2. g function (universal subleading constant of Renyi entropy) for complete dephasing channel $\mathcal{D}_{p=1,\vec{v}}$ applied to critical Ising ground state, where $\vec{v} = [\sin(\pi\tilde{\theta}/2), 0, \cos(\pi\tilde{\theta}/2)]$ in the XZ plane. Left: $g(\tilde{\theta}, L)$ for different L (legend). Right: data collapse for $0 \le \tilde{\theta} \le 0.6$, indicating RG flow from $\mathcal{D}_z$ to $\mathcal{D}_{zx}$.

operator in the n-copied CFT. Thus, $\Delta_O^{(n)}$ must be a sum of n scaling dimensions in the original CFT.

Critical Ising model under dephasing noise.—As an example, we study the effect of dephasing noise on the ground state of the 1D transverse-field Ising model:

$$H = -\sum_{i=1}^{L} \sigma_{x,i}\sigma_{x,i+1} - \sum_{i=1}^{L} \sigma_{z,i}. \tag{14}$$

For the dephasing noise $\mathcal{D}_{p,\vec{v}}$, we restrict the direction to the XZ plane, i.e., $\vec{v} = [\sin(\pi\tilde{\theta}/2), 0, \cos(\pi\tilde{\theta}/2)]$, where $0 \le \tilde{\theta} \le 1$. For Renyi index $n = 2$, we find four RG fixed points: (1) identity channel $\mathcal{I} = \mathcal{D}_{0,\vec{v}}$, with $\log g_{\mathcal{I}} = 0$, (2) complete dephasing in Z direction $\mathcal{D}_z$, with $\log g_z = 0$, (3) complete dephasing in X direction $\mathcal{D}_x$, with $\log g_x = -\log 2$, and (4) complete dephasing $\mathcal{D}_{zx}$ at $\tilde{\theta} \approx 0.8$, with $\log g_{zx} = -2\log 2$. For complete dephasing, the entropy reduces to the "classical Shannon entropy" of Ref. [56], which considered cases (2) and (3).

We also observe the RG flow between these four fixed points, which manifests the monotonicity of the g function. Near the $\mathcal{D}_z$, $\mathcal{D}_x$ fixed points, we can turn on a small perturbation to $\tilde{\theta}$ and observe the RG flows to the $\mathcal{D}_{zx}$ fixed point. The universal data collapses indicate the critical exponents $\nu \approx 2.0$, 1.0 for the two respective channels; see Fig. 2 and Ref. [36]. Another example is the RG flow from $\mathcal{I}$ fixed point to complete dephasing $\mathcal{D}_{zx}$ and $\mathcal{D}_x$ by turning on a small p [36]. Finally, all dephasing channels $\mathcal{D}_{p,z}$ have the same $\log g = 0$, which suggests they constitute a continuous family of fixed points connected by marginal deformations. These RG flows are summarized in Fig. 3. We have also checked that the RG flows in this example are the same for higher Renyi indices such as $n = 3$, although consistency between Renyi indices is not *a priori* true [57].

The mutual information between subsystems at the four RG fixed points is shown in Fig. 3. For complementary intervals, we find that they all satisfy Eq. (12) with the same $\Delta_{\mathcal{IN}}^{(2)} = 1/16$. For the identity channel, the operator $\phi_{\mathcal{IN}}^{(2)}$ is the branch-point twist operator, with the scaling dimension $c/8 = 1/16$. The fact that the scaling dimensions coincide for dephasing channel and identity channel was also observed numerically in Ref. [58]. In order to distinguish the channels, we compute the Renyi mutual information $I^{(n)}(A, B)$ of two disjoint intervals. We see that the scaling dimensions of $\Delta_O^{(2)}$ vary among the four fixed points. These dimensions can be understood analytically in terms of local operators in the two-copied Ising model [36].

Finally, we study the Renyi negativity $N_A^{(3)}$ of a subsystem A under dephasing noise; see Fig. 4. For Z dephasing, we find a logarithmic scaling with continuously changing coefficients, which is an indication of a continuous set of RG fixed points. For X dephasing, even with a small strength p, the Renyi negativity obeys an area law, in agreement with the previous observation that the channel flows to complete dephasing. We also observe that a weak Y dephasing is an irrelevant perturbation, indicated by both the g function and the scaling of $I^{(2)}(A, \bar{A})$ and $N^{(3)}(A, \bar{A})$. Indeed, we find in Fig. 4 that for Y dephasing with small p, the coefficient of the log scaling of negativity does not change with respect to the initial pure critical state, i.e., the one with $\mathcal{I}$ channel.

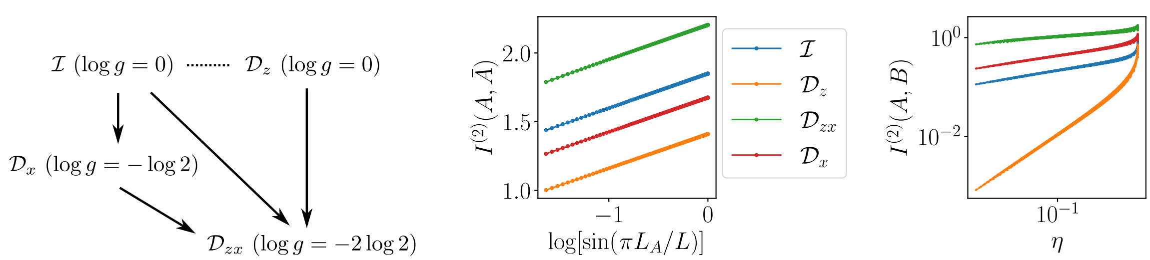

FIG. 3. Fixed-point channels for Ising model and their universal properties. Left: g function of the four fixed points among dephasing channels and their RG flow. The dashed line indicates a continuous set of fixed points and the solid lines indicate direction of the RG flow. Center: $I^{(2)}(A, \bar{A})$ of a single interval at the four fixed points. All four slopes are estimated to be close to $4\Delta_{\mathcal{IN}}^{(2)} \approx 1/4$. Right: $I^{(2)}(A, B)$ of a two disjoint intervals at the four fixed points. The scaling dimension $\Delta_O^{(2)}$ is close to $1/4, 1, 1/8, 1/4$ for the four fixed points $\mathcal{I}, \mathcal{D}_z, \mathcal{D}_{zx}, \mathcal{D}_x$, respectively.

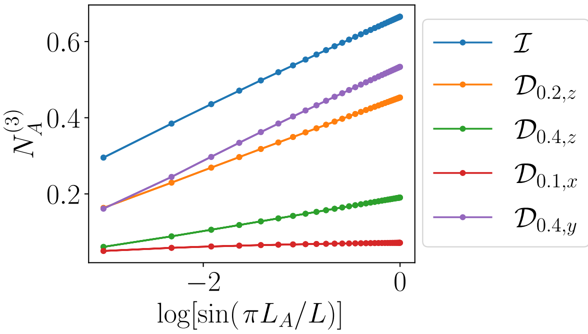

FIG. 4. Renyi negativity $N_A^{(3)}$ of a subsystem A for the ground state of critical Ising model ($L = 64$) under various choices of dephasing noise. Dephasing in x, y, z directions are, respectively, relevant, irrelevant, and marginal perturbations, implying that the negativity scaling is, respectively, area law or log scaling with either the same coefficient as the initial pure critical state or continuously changing with strength p.

Discussion.—In this work we have established a notion of RG flow between quantum channels acting on a critical wave function, and we have demonstrated its consequences on the entanglement structure of the resulting mixed states. We have shown that a g function gives the volume-independent part of the Renyi entropy at the RG fixed points and established its monotonicity under the RG flow. We have illustrated all this in the example of the transverse-field Ising model under dephasing noise, although generalization to other noise models such as depolarizing noise is straightforward and also yields interesting phenomena (see Ref. [36] for details).

Our notion of RG flow can be naturally applied to measurement-induced quantities of a critical wave function, such as those considered in Refs. [25,26]. Another direction is to classify the conformal boundary conditions for the fixed-point quantum channels in the CFT and take the replica limit, along the lines of Ref. [59]. Regarding the holographic correspondence between a CFT on the boundary of a spacetime and a gravitational theory in the bulk, it would be interesting to explore the holographic dual of quantum channels acting on the boundary; many recent works have considered coupling the boundary CFT to a bath, and perhaps our formalism could be related to replica wormholes [60–62]. In another direction, while this work only considered one layer of local quantum channels, it may also be interesting to explore the entanglement dynamics of random local channels [37] on quantum critical (and other long-range entangled) states.

Finally, we discuss the experimental relevance of our work. Quantum critical states have already been realized on programmable quantum simulators (see, e.g., Refs. [8,38] for the realization of a critical transverse-field Ising ground state), and such platforms may be naturally subject to biased noise in which one type of channel (e.g., dephasing in a particular direction) dominates (see Refs. [63–65] for details on different hardwares). Alternatively, the noise channels can also be realized by local unitary gates acting on system and ancillas. The entanglement properties (Renyi entropy and negativity) of the resulting mixed states can be probed using recent techniques of shadow tomography [39,40] which use randomized measurements to estimate moments of a (partially transposed) density matrix. Our predictions can be realized on near-term quantum simulators, and we discuss the experimental setup in detail in Ref. [36].

We thank Runze Chi, Soonwon Choi, Paolo Glorioso, Vedika Khemani, Yaodong Li, Yuhan Liu, Peter Lu, Alex May, Xiao-Liang Qi, Guifre Vidal, Jinzhao Wang, and Fei Yan for helpful discussions. Y. Z. particularly thanks Ehud Altman, Samuel Garatt, and Zack Weinstein for explanation of their work Ref. [26]. We thank Jacob Lin and Weicheng Ye for collaboration on a related project. S. S. and T. H. H. are supported by Perimeter Institute and NSERC. Research at Perimeter Institute is supported in part by the Government of Canada through the Department of Innovation, Science and Economic Development Canada and by the Province of Ontario through the Ministry of Colleges and Universities. Y. Z. is supported by the Q-FARM fellowship at Stanford University.

Note added.—Recently, we noticed a related independent work [66].

[1] F. Arute *et al.*, Quantum supremacy using a programmable superconducting processor, Nature (London) **574**, 505 (2019).

[2] H.-S. Zhong *et al.*, Quantum computational advantage using photons, Science **370**, 1460 (2020).

[3] L. S. Madsen, F. Laudenbach, M. F. Askarani, F. Rortais, T. Vincent, J. F. F. Bulmer, F. M. Miatto, L. Neuhaus, L. G. Helt, M. J. Collins, A. E. Lita, T. Gerrits, S. W. Nam, V. D. Vaidya, M. Menotti, I. Dhand, Z. Vernon, N. Quesada, and J. Lavoie, Quantum computational advantage with a programmable photonic processor, Nature (London) **606**, 75 (2022).

[4] J. Zhang, G. Pagano, P. W. Hess, A. Kyprianidis, P. Becker, H. Kaplan, A. V. Gorshkov, Z. X. Gong, and C. Monroe, Observation of a many-body dynamical phase transition with a 53-qubit quantum simulator, Nature (London) **551**, 601 (2017).

[5] H. Bernien, S. Schwartz, A. Keesling, H. Levine, A. Omran, H. Pichler, S. Choi, A. S. Zibrov, M. Endres, M. Greiner, V. Vuletić, and M. D. Lukin, Probing many-body dynamics on a 51-atom quantum simulator, Nature (London) **551**, 579 (2017).

[6] G. Semeghini, H. Levine, A. Keesling, S. Ebadi, T. T. Wang, D. Bluvstein, R. Verresen, H. Pichler, M. Kalinowski, R. Samajdar, A. Omran, S. Sachdev, A. Vishwanath, M. Greiner, V. Vuletić, and M. D. Lukin, Probing topological spin liquids on a programmable quantum simulator, Science **374**, 1242 (2021).

[7] K. J. Satzinger *et al.*, Realizing topologically ordered states on a quantum processor, Science **374**, 1237 (2021).

[8] D. Zhu, S. Johri, N. M. Linke, K. A. Landsman, C. Huerta Alderete, N. H. Nguyen, A. Y. Matsuura, T. H. Hsieh, and C. Monroe, Generation of thermofield double states and critical ground states with a quantum computer, Proc. Natl. Acad. Sci. U.S.A. **117**, 25402 (2020).

[9] B. Skinner, J. Ruhman, and A. Nahum, Measurement-Induced Phase Transitions in the Dynamics of Entanglement, Phys. Rev. X **9**, 031009 (2019).

[10] A. Chan, R. M. Nandkishore, M. Pretko, and G. Smith, Unitary-projective entanglement dynamics, Phys. Rev. B **99**, 224307 (2019).

[11] Y. Li, X. Chen, and M. P. A. Fisher, Quantum Zeno effect and the many-body entanglement transition, Phys. Rev. B **98**, 205136 (2018).

[12] S. Choi, Y. Bao, X.-L. Qi, and E. Altman, Quantum Error Correction in Scrambling Dynamics and Measurement-Induced Phase Transition, Phys. Rev. Lett. **125**, 030505 (2020).

[13] M. J. Gullans and D. A. Huse, Dynamical Purification Phase Transition Induced by Quantum Measurements, Phys. Rev. X **10**, 041020 (2020).

[14] C.-M. Jian, Y.-Z. You, R. Vasseur, and A. W. W. Ludwig, Measurement-induced criticality in random quantum circuits, Phys. Rev. B **101**, 104302 (2020).

[15] Y. Bao, S. Choi, and E. Altman, Theory of the phase transition in random unitary circuits with measurements, Phys. Rev. B **101**, 104301 (2020).

[16] C. de Groot, A. Turzillo, and N. Schuch, Symmetry protected topological order in open quantum systems, Quantum **6**, 856 (2022).

[17] R. Ma and C. Wang, Average symmetry-protected topological phases, arXiv:2209.02723.

[18] J. Y. Lee, Y.-Z. You, and C. Xu, Symmetry protected topological phases under decoherence, arXiv:2210.16323.

[19] E. Lake, S. Balasubramanian, and S. Choi, Exact quantum algorithms for quantum phase recognition: Renormalization group and error correction, arXiv:2211.09803.

[20] R. Fan, Y. Bao, E. Altman, and A. Vishwanath, Diagnostics of mixed-state topological order and breakdown of quantum memory, arXiv:2301.05689.

[21] Y. Bao, R. Fan, A. Vishwanath, and E. Altman, Mixed-state topological order and the errorfield double formulation of decoherence-induced transitions, arXiv:2301.05687.

[22] J.-H. Zhang, Y. Qi, and Z. Bi, Strange correlation function for average symmetry-protected topological phases, arXiv: 2210.17485.

[23] J. Behrends, F. Venn, and B. Béri, Surface codes, quantum circuits, and entanglement phases, arXiv:2212.08084.

[24] M. A. Rajabpour, Entanglement entropy after a partial projective measurement in $1+1$ dimensional conformal field theories: Exact results, J. Stat. Mech. 6 (2016) 063109.

[25] C.-J. Lin, W. Ye, Y. Zou, S. Sang, and T. H. Hsieh, Probing sign structure using measurement-induced entanglement, Quantum **7**, 910 (2023).

[26] S. J. Garratt, Z. Weinstein, and E. Altman, Measurements Conspire Nonlocally to Restructure Critical Quantum States, Phys. Rev. X **13**, 021026 (2023).

[27] S. Antonini, G. Bentsen, C. Cao, J. Harper, S.-K. Jian, and B. Swingle, Holographic measurement and bulk teleportation, J. High Energy Phys. 12 (2022) 124.

[28] J. Preskill, *Lecture Notes for Physics 229: Quantum Information and Computation* (California Institute of Technology, Pasadena, 1998).

[29] M. Oshikawa and I. Affleck, Boundary conformal field theory approach to the critical two-dimensional Ising model with a defect line, Nucl. Phys. **B495**, 533 (1997).

[30] G. Vidal and R. F. Werner, Computable measure of entanglement, Phys. Rev. A **65**, 032314 (2002).

[31] P. Calabrese, J. Cardy, and E. Tonni, Entanglement Negativity in Quantum Field Theory, Phys. Rev. Lett. **109**, 130502 (2012).

[32] P. Calabrese and J. Cardy, Time Dependence of Correlation Functions Following a Quantum Quench, Phys. Rev. Lett. **96**, 136801 (2006).

[33] P. Calabrese and J. Cardy, Quantum quenches in extended systems, J. Stat. Mech. (2007) P06008.

[34] P. Calabrese and J. Cardy, Quantum quenches in 1 dimensional conformal field theories, J. Stat. Mech. (2016) 064003.

[35] J. Cardy, Bulk renormalization group flows and boundary states in conformal field theories, SciPost Phys. **3**, 011 (2017).

[36] See Supplemental Material at http://link.aps.org/supplemental/10.1103/PhysRevLett.130.250403 for more comments on the applicability of conformal boundary conditions to quantum quench problems, other examples of dephasing channels and a detailed discussion of the experimental protocol, which includes Refs. [8,35,37–47].

[37] Z. Li, S. Sang, and T. H. Hsieh, Entanglement dynamics of random quantum channels, Phys. Rev. B **107**, 014307 (2023).

[38] S. Anand, J. Hauschild, Y. Zhang, A. C. Potter, and M. P. Zaletel, Holographic quantum simulation of entanglement renormalization circuits, arXiv:2203.00886.

[39] H.-Y. Huang, R. Kueng, and J. Preskill, Predicting many properties of a quantum system from very few measurements, Nat. Phys. **16**, 1050 (2020).

[40] A. Elben, R. Kueng, H.-Y. R. Huang, R. van Bijnen, C. Kokail, M. Dalmonte, P. Calabrese, B. Kraus, J. Preskill, P. Zoller, and B. Vermersch, Mixed-State Entanglement from Local Randomized Measurements, Phys. Rev. Lett. **125**, 200501 (2020).

[41] H. Shapourian, K. Shiozaki, and S. Ryu, Partial time-reversal transformation and entanglement negativity in fermionic systems, Phys. Rev. B **95**, 165101 (2017).

[42] Y. Liu, R. Sohal, J. Kudler-Flam, and S. Ryu, Multipartitioning topological phases by vertex states and quantum entanglement, Phys. Rev. B **105**, 115107 (2022).

[43] Y. Zou, A. Milsted, and G. Vidal, Conformal Fields and Operator Product Expansion in Critical Quantum Spin Chains, Phys. Rev. Lett. **124**, 040604 (2020).

[44] H. Shapourian and S. Ryu, Entanglement negativity of fermions: Monotonicity, separability criterion, and classification of few-mode states, Phys. Rev. A **99**, 022310 (2019).

[45] H. Shapourian, P. Ruggiero, S. Ryu, and P. Calabrese, Twisted and untwisted negativity spectrum of free fermions, SciPost Phys. **7**, 037 (2019).

[46] S. Murciano, V. Vitale, M. Dalmonte, and P. Calabrese, Negativity Hamiltonian: An Operator Characterization of Mixed-State Entanglement, Phys. Rev. Lett. **128**, 140502 (2022).

[47] W. W. Ho and T. H. Hsieh, Efficient variational simulation of non-trivial quantum states, SciPost Phys. **6**, 029 (2019).

[48] D. Friedan and A. Konechny, Boundary Entropy of One-Dimensional Quantum Systems at Low Temperature, Phys. Rev. Lett. **93**, 030402 (2004).

[49] H. Casini, I. S. Landea, and G. Torroba, The g-theorem and quantum information theory, J. High Energy Phys. 10 (2016) 140.

[50] G. Cuomo, Z. Komargodski, and A. Raviv-Moshe, Renormalization Group Flows on Line Defects, Phys. Rev. Lett. **128**, 021603 (2022).

[51] I. Affleck and A. W. W. Ludwig, Universal Noninteger "Ground State Degeneracy" in Critical Quantum Systems, Phys. Rev. Lett. **67**, 161 (1991).

[52] I. Affleck, Boundary condition changing operations in conformal field theory and condensed matter physics, Nucl. Phys. B, Proc. Suppl. **58**, 35 (1997), Proceedings of the European Research Conference in the Memory of Claude Itzykson.

[53] Y. Li, X. Chen, A. W. W. Ludwig, and M. P. A. Fisher, Conformal invariance and quantum nonlocality in critical hybrid circuits, Phys. Rev. B **104**, 104305 (2021).

[54] P. Calabrese, C. Hagendorf, and P. L. Doussal, Time evolution of one-dimensional gapless models from a domain wall initial state: Stochastic Loewner evolution continued?, J. Stat. Mech. (2008) P07013.

[55] The coefficient $\alpha^{(n)}$ can be understood as the line tension of creating the domain wall. It is a nonuniversal constant that depends on details of the lattice realization.

[56] J.-M. Stéphan, S. Furukawa, G. Misguich, and V. Pasquier, Shannon and entanglement entropies of one- and two-dimensional critical wave functions, Phys. Rev. B **80**, 184421 (2009).

[57] We have observed consistency also for the dephasing in Y direction, which appears to be an irrelevant perturbation for both $n = 2$ and $n = 3$.

[58] F. C. Alcaraz and M. A. Rajabpour, Universal Behavior of the Shannon Mutual Information of Critical Quantum Chains, Phys. Rev. Lett. **111**, 017201 (2013).

[59] T. Quella, I. Runkel, and G. M. Watts, Reflection and transmission for conformal defects, J. High Energy Phys. 04 (2007) 095.

[60] A. Almheiri, N. Engelhardt, D. Marolf, and H. Maxfield, The entropy of bulk quantum fields and the entanglement wedge of an evaporating black hole, J. High Energy Phys. 12 (2019) 063.

[61] G. Penington, S. H. Shenker, D. Stanford, and Z. Yang, Replica wormholes and the black hole interior, J. High Energy Phys. 03 (2022) 205.

[62] A. Almheiri, T. Hartman, J. Maldacena, E. Shaghoulian, and A. Tajdini, Replica wormholes and the entropy of Hawking radiation, J. High Energy Phys. 063 (2020) 013.

[63] A. A. Clerk, M. H. Devoret, S. M. Girvin, F. Marquardt, and R. J. Schoelkopf, Introduction to quantum noise, measurement, and amplification, Rev. Mod. Phys. **82**, 1155 (2010).

[64] P. Aliferis, F. Brito, D. P. DiVincenzo, J. Preskill, M. Steffen, and B. M. Terhal, Fault-tolerant computing with biased-noise superconducting qubits: A case study, New J. Phys. **11**, 013061 (2009).

[65] D. Nigg, M. Müller, E. A. Martinez, P. Schindler, M. Hennrich, T. Monz, M. A. Martin-Delgado, and R. Blatt, Quantum computations on a topologically encoded qubit, Science **345**, 302 (2014).

[66] J. Y. Lee, C.-M. Jian, and C. Xu, Quantum criticality under decoherence or weak measurement, arXiv:2301.05238.